High Cytotoxicity of Cisplatin Nanocapsules in Ovarian Carcinoma Cells Depends on Uptake by Caveolae-Mediated Endocytosis

Irene H.L. Hamelers,[1,2] Rutger W.H.M. Staffhorst,[1] Jarno Voortman,[3] Ben de Kruijff,[1] Jan Reedijk,[4] Paul M.P. van Bergen en Henegouwen,[3] and Anton I.P.M. de Kroon[1,2]

Abstract

Purpose: Cisplatin nanocapsules, nanoprecipitates of cisplatin encapsulated in phospholipid bilayers, exhibit increased *in vitro* toxicity compared with the free drug toward a panel of human ovarian carcinoma cell lines. To elucidate the mechanism of cell killing by nanocapsules and to understand the cell line dependence of nanocapsule efficacy, the route of uptake and the intracellular fate of the nanocapsules were investigated.

Experimental Design: Intracellular platinum accumulation and cisplatin-DNA-adduct formation were measured in cell lines that differ in sensitivity to cisplatin nanocapsules. Confocal fluorescence microscopy in combination with down-regulation with small interfering RNA was used to map the route of cellular uptake of nanocapsules containing fluorescein-labeled cisplatin.

Results: In sensitive cell lines, cisplatin from nanocapsules is taken up much more efficiently than the free compound. In IGROV-1 cells, the increased platinum accumulation results in augmented cisplatin-DNA-adduct formation. Confocal fluorescence microscopy revealed that the uptake of nanocapsules is energy dependent. Colocalization with markers of early and late endosomes indicated uptake via endocytosis. Down-regulation of caveolin-1 with small interfering RNA inhibited the uptake and cytotoxic effect of nanocapsules in IGROV-1 cells. Ovarian carcinoma cells, in which the nanocapsules are less effective than in IGROV-1 cells, do not internalize the nanocapsules (OVCAR-3) or accumulate them in an endocytic compartment after clathrin-mediated endocytosis (A2780).

Conclusions: The high cytotoxicity of cisplatin nanocapsules requires caveolin-1-dependent endocytosis that is followed by release of the drug from a late endosomal/lysosomal compartment and cisplatin-DNA-adduct formation. The findings may be applied in predicting the efficacy of nanoparticulate anticancer drug delivery systems in treating different tumor types.

Platinum-based drugs are established in the treatment of cancer, including ovarian, head and neck, and lung cancer (1). The oldest and most commonly used platinum-based drug, *cis*-diamminedichloroplatinum[II] (cisplatin), is activated via hydrolysis, yielding positively charged, very reactive aquated species that subsequently can form stable DNA-adducts and as a consequence cause cell death (1). Common problems associated with the clinical use of cisplatin are cumulative toxicities, such as nephrotoxicity, ototoxicity, and peripheral neuropathy (2). In addition, the rapid inactivation due to coordination to tissue and plasma proteins and the occurrence of inherent or treatment-induced resistant tumor cell subpopulations limit the therapeutic efficacy of cisplatin (1). One of the strategies to reduce the systemic toxicity and to prevent inactivation of platinum drugs in the bloodstream and tissue fluid is the encapsulation of the drug in liposomes (3). Two liposomal formulations of cisplatin, SPI-077 and Lipoplatin, have been tested in clinical trials. SPI-077 was found to exhibit essentially no antitumor activity in patients in phase I and II studies (4–6), whereas Lipoplatin exhibited reduced side effects compared with cisplatin in a phase I study (7) and is currently in a phase III trial.

A major problem associated with the liposomal formulations of cisplatin is the limited bioavailability of the drug in the tumor (5, 8). Key factors are likely the low water solubility (8 mmol/L at 37°C) and low lipophilicity of cisplatin (9), which lead to liposomal formulations with low drug-to-lipid molar ratios (in the order of 0.05 mol platinum/mol lipid). Previously, an alternative method was developed to encapsulate cisplatin in a lipid formulation with superior efficiency (10). This method takes advantage of the limited solubility of the drug in water. Repeated freezing and thawing of an equimolar

Authors' Affiliations: [1]Biochemistry of Membranes and [2]Membrane Enzymology, Bijvoet Institute and Institute of Biomembranes, and [3]Department of Cellular Architecture and Dynamics, Institute of Biomembranes, Utrecht University, Utrecht, The Netherlands and [4]Leiden Institute of Chemistry, Leiden University, Leiden, The Netherlands

Received 7/3/08; revised 9/17/08; accepted 9/22/08.

Grant support: Dutch Cancer Society (KWF Kankerbestrijding) and NanoNed, a national nanotechnology program coordinated by the Dutch Ministry of Economic Affairs.

The costs of publication of this article were defrayed in part by the payment of page charges. This article must therefore be hereby marked *advertisement* in accordance with 18 U.S.C. Section 1734 solely to indicate this fact.

Note: Supplementary data for this article are available at Clinical Cancer Research Online (http://clincancerres.aacrjournals.org/).

Requests for reprints: Anton I.P.M. de Kroon, Membrane Enzymology, Bijvoet Institute and Institute of Biomembranes, Utrecht University, Padualaan 8, 3584 CH Utrecht, The Netherlands. Phone: 31-30-2533424; Fax: 31-30-2522478; E-mail: a.i.p.m.dekroon@uu.nl.

doi:10.1158/1078-0432.CCR-08-1702

Translational Relevance

Cisplatin nanocapsules represent a lipid formulation of cisplatin with unsurpassed encapsulation efficiency and cell killing ability *in vitro*. Here, we show that the cytotoxicity of cisplatin nanocapsules in human ovarian carcinoma cells strictly depends on the uptake of the particles via caveolin-1-mediated endocytosis. Reduced drug uptake is a major cause of cisplatin resistance in cancer cell lines and tumors. The cisplatin nanocapsules may circumvent the mechanisms leading to the reduced drug accumulation and thus kill platinum-resistant cells. Recent data suggest that nanocapsules can overcome platinum resistance *in vitro*. Moreover, the dependence of the cytotoxicity on the route of cellular entry established for cisplatin nanocapsules may provide a new strategy for predicting the efficacy of nanoparticulate anticancer drug delivery systems against different types of tumors.

dispersion of zwitterionic 1,2-dioleoyl-*sn*-glycero-3-phosphocholine and anionic 1,2-dioleoyl-*sn*-glycero-3-phosphoserine in a concentrated aqueous solution of cisplatin yielded cisplatin nanocapsules, aggregates of cisplatin surrounded by a single lipid bilayer. Solid-state nuclear magnetic resonance analysis of the architecture of the nanocapsules revealed that the core consists of solid cisplatin: 90% as the starting dichlorido species and 10% as a positively charged chloride-bridged dinuclear species (11). The cisplatin nanocapsules have an unprecedented drug-to-lipid molar ratio (11:1) and *in vitro* cytotoxicity toward IGROV-1 cells, with the IC_{50} being two orders of magnitude lower than that of the free drug (10). The limited stability of 1,2-dioleoyl-*sn*-glycero-3-phosphocholine/1,2-dioleoyl-*sn*-glycero-3-phosphoserine cisplatin nanocapsules in serum was improved by the incorporation of cholesterol and polyethylene glycol-modified lipids (12).

In the present study, the origin of the enhanced cytotoxicity of the cisplatin nanocapsules was addressed by determining cellular platinum accumulation, platinum-DNA-adduct formation, and by studying the interaction of fluorescently labeled nanocapsules with the cells using confocal fluorescence microscopy. A panel of human ovarian carcinoma cell lines was tested for sensitivity to cisplatin nanocapsules compared with the free drug, revealing that the increase in cytotoxicity varied between cell lines. To explain the cell line dependence of nanocapsule efficacy, the route of uptake and intracellular fate of the cisplatin encapsulated in nanocapsules was investigated in three ovarian carcinoma cell lines that respond differently to cisplatin nanocapsules.

Materials and Methods

Preparation of cisplatin nanocapsules. Cisplatin nanocapsules were prepared as described before (10), with slight modifications. In brief, cisplatin (ABCR GmbH & Co.), dissolved at 5 mmol/L in MilliQ water, was used to hydrate a dry phospholipid film consisting of an equimolar mixture of 1,2-dioleoyl-*sn*-glycero-3-phosphocholine and 1,2-dioleoyl-*sn*-glycero-3-phosphoserine (Avanti Polar Lipids). The lipid dispersion (1.2 mmol/L phospholipid) was incubated at 37°C for 30 min and then subjected to 10 freeze-thaw cycles using ethanol/dry ice (-70°C) and a water bath at 37°C. Nonencapsulated cisplatin was removed by centrifugation (twice for 4 min at 500 × *g*, room temperature). The pellet was resuspended in MilliQ, incubated for 2 h at 37°C, and washed again. This additional incubation was found to improve the reproducibility of the cytotoxicity of the cisplatin nanocapsules (data not shown). Platinum content was quantified by non-flame atomic absorption spectroscopy and phospholipid-content was quantified by phosphate analysis as described (13). Cisplatin nanocapsules exhibit a heterogeneous size distribution with 75% of the population having a width ~50 nm and a length between 50 and 250 nm (13).

For preparation of double-labeled fluorescent nanocapsules, 0.5 mol% carboxyfluorescein-labeled cisplatin (CF-cisplatin) was added to the cisplatin solution and 0.2 mol% 2-(4,4-difluoro-5-(4-phenyl-1,3-butadienyl)-4-bora-3a,4a-diaza-*s*-indacene-3-pentanoyl)-1-hexadecanoyl-*sn*-glycero-3-phosphocholine (C5-Bodipy 581-PC; Molecular Probes/Invitrogen) was included in the lipid film. The CF-cisplatin was prepared from carboxyfluorescein diacetate (CFDA)-cisplatin (14) by hydrolyzing the acetate esters by overnight incubation at 37°C in TBS (pH 8.95).

Cell culture. The IGROV-1, A2780, and OVCAR-3 cell lines were maintained in RPMI 1640 (Invitrogen) containing 10% FCS Gold (PAA Laboratories) and 100 units/mL penicillin and 100 μg/mL streptomycin. SK-OV-3 was cultured in DMEM (Invitrogen) with 10% FCS Gold, 100 units/mL penicillin, and 100 μg/mL streptomycin.

In vitro *cytotoxicity assay.* Cytotoxicity was assayed as described (10). In short, ~500 to 1,000 human carcinoma cells were seeded per well in a 96-well plate (Costar) in 200 μL culture medium. After 24 h, cisplatin formulations were added, and the cells were incubated for 3 days at 37°C. Tumor cell survival was measured using a sulforhodamine B assay (15). The data were fitted to a sigmoidal dose-response curve (variable slope) using GraphPad Prism (GraphPad Software).

Quantification of intracellular platinum accumulation and DNA-adduct formation. Approximately 10^7 cells of the cell line indicated were incubated for 2 h at 37°C with free cisplatin or cisplatin nanocapsules at the concentrations indicated. The cells were washed twice with ice-cold PBS, harvested by scraping in ice-cold PBS, and centrifuged. A sample was taken for protein determination according to Bradford (16). The cell pellet was digested in 65% (v/v) nitric acid at 75°C for 2 h. After appropriate dilution in water, platinum content was analyzed by non-flame atomic absorption spectroscopy. Cellular platinum levels were expressed in ng platinum/mg protein.

Cisplatin-DNA-adduct formation was measured using ~3×10^7 cells per condition. The cells were incubated at 37°C with free cisplatin or cisplatin nanocapsules for 5 min or 4 h at final concentrations of 50 μmol/L cisplatin. Next, the cells were washed twice with ice-cold PBS, detached with trypsin/EDTA (Invitrogen), and diluted in RPMI 1640 containing 10% FCS. Cells were pelleted by centrifugation and the medium was removed leaving behind ~300 μL residual liquid. DNA was isolated with the Puregene DNA Purification Kit (Gentra Systems) according to the manufacturer's instructions. DNA concentrations and 260/280 ratios were determined spectrophotometrically. Only samples with a 260/280 ratio higher than 1.7 were analyzed for platinum. The isolated DNA was digested with DNase I before analysis of platinum content by non-flame atomic absorption spectroscopy as described (17). Total DNA-adducts were expressed in pg platinum/μg DNA. To verify that the platinum isolated in the assay was coordinated to the DNA, the amount of platinum coisolated with DNA was determined 5 min after addition of free and encapsulated cisplatin to the cells: no platinum was detected in these samples (data not shown).

Confocal fluorescence microscopy. Cells were seeded on sterile glass coverslips in culture medium. Twenty-four hours after seeding, the cells were incubated for the periods indicated at 37°C with free cisplatin spiked with 0.5 mol% CF-cisplatin or CFDA-cisplatin or double-labeled fluorescent nanocapsules at a final cisplatin concentration of 50 μmol/L. Subsequently, cells were washed with PBS and fixed with 4% paraformaldehyde for 15 min. After fixation, the cells were permeabilized

with 0.1% Triton X-100 in PBS for 5 min and blocked with 2% bovine serum albumin in PBS for 1 h at room temperature. The coverslips were then stained with the appropriate antibodies (18–20) as described previously (21). After staining, the coverslips were mounted in Mowiol/Dabco (Calbiochem/Sigma-Aldrich). Images were collected by confocal microscopy (Nikon C1 microscope). Settings of the Nikon imaging software (laser strength and gain) were kept constant within each experiment to allow for comparison of the overall fluorescence intensities of samples.

Transfection of small interfering RNA. The small interfering RNAs (siRNA) used were 5′-GCAGAACCAGAAGGGACACACAGUU-3′ for knockdown of caveolin-1 (starting from nucleotide 495; based on ref. 22), 5′-CCAUCUUCUUAACCCUGAGUGGUUA-3′ for clathrin heavy chain (CHC; starting from nucleotide 252; based on ref. 23), and 5′-CCUUGACGUCAUAGUCAUUUGUGGA-3′ as scrambled negative control (23) and were all obtained from Invitrogen. Cells were used for transfection at 15% to 30% confluency in 12-well plates, each well containing 1 mL 10% FCS in RPMI 1640. For each transfection sample, 2 μL Lipofectamine 2000 (Invitrogen) was added to 100 μL Opti-MEM I (Invitrogen) and incubated at room temperature for 5 min. The diluted Lipofectamine was added to a second solution of 100 μL Opti-MEM I containing 75 pmol siRNA and incubated at room temperature for 20 min after mixing. Subsequently, the transfection mixtures were added drop-wise to each well. After 3 days, the cells were reseeded for use in experiments on day 4. Cells treated with Lipofectamine served as the mock-treated control. In each experiment, the knockdown was verified by Western blotting using antibodies against caveolin and CHC (both from Transduction Laboratories). For this purpose, cells were solubilized in lysis buffer [62.5 mmol/L Tris-HCl (pH 6.8), 10% glycerol, 2% SDS], and aliquots of the cell lysates corresponding to 20 μg protein as measured by the BCA method (Pierce) with bovine serum albumin as a standard, were supplemented with 2.5% 2-mercaptoethanol and 0.01% bromophenol blue, incubated at 95°C for 5 min, and separated by SDS-PAGE.

Results

Enhancement of the cytotoxicity of cisplatin by encapsulation in nanocapsules is cell line dependent. Previously, cisplatin nanocapsules were shown to be 2 orders of magnitude more cytotoxic than the free drug toward IGROV-1 cells in an *in vitro* cytotoxicity assay (10). To investigate whether the encapsulation of cisplatin in nanocapsules leads to a general improvement of the efficacy of the drug, we assayed the cytotoxicity of the nanocapsules toward a panel of human ovarian carcinoma cell lines commonly used in testing platinum drugs (24–26) and compared the IC_{50} value of the nanocapsules with that of the free drug (Table 1). Similar to IGROV-1, the SK-OV-3 cell line was found to be >100-fold more sensitive to cisplatin nanocapsules than to the free drug. The A2780 cell line was slightly more effectively killed by cisplatin nanocapsules than by free cisplatin, whereas, remarkably, the nanocapsules did not show improved cytotoxicity toward OVCAR-3 cells.

Cisplatin from nanocapsules is taken up more efficiently than free cisplatin. To elucidate the mechanism of the enhanced cytotoxicity of cisplatin nanocapsules, the intracellular platinum accumulation was measured by non-flame atomic absorption spectroscopy (Fig. 1A). The platinum accumulation in IGROV-1 cells treated with cisplatin nanocapsules was much higher than in cells treated with the free drug, with the platinum accumulation in cells treated with 0.5 μmol/L cisplatin nanocapsules being comparable with the platinum accumulation in cells treated with 50 μmol/L free cisplatin. This result indicates that the increased efficacy of cisplatin encapsulated in nanocapsules toward IGROV-1 cells could be caused by increased platinum accumulation in the cells.

Although cellular platinum accumulation after treatment with the free drug varies somewhat between cell lines (Fig. 1B), platinum accumulation increased when cisplatin nanocapsules were used. Overall, a good correlation is observed between the increased uptake of platinum and the cytotoxicity of the nanocapsules, with the largest increases in the most sensitive cell lines, IGROV-1 and SK-OV-3 cells, and the smallest increase in the OVCAR-3 cells, which are the least sensitive. The data suggest that the efficiency of uptake of the nanocapsules determines the sensitivity of the cell lines tested, with one exception. Interestingly, the A2780 cell line accumulates much more platinum than expected based on the cytotoxicity of the nanocapsules (Table 1; Fig. 1B).

Cytotoxicity of cisplatin nanocapsules is reflected by the amount of platinum-DNA-adducts formed rather than by the intracellular platinum accumulation. Treatment of cells and tumors with conventional cisplatin results in the formation of DNA-adducts that interfere with transcription and replication, eventually causing apoptosis (1). To examine whether the uptake of cisplatin from nanocapsules leads to formation of platinum-DNA-adducts, DNA-associated platinum was assayed in three cell lines with different responses to cisplatin nanocapsules, IGROV-1, A2780, and OVCAR-3 (Fig. 1C). After 4 h of incubation, 22 pg platinum/μg DNA was detected in IGROV-1 cells treated with 50 μmol/L free cisplatin, which is comparable with published data (27). On treatment with cisplatin nanocapsules, 5-fold more platinum was found coordinated to the DNA in IGROV-1 cells (Fig. 1C), whereas in A2780 and OVCAR-3 cells the platinum-DNA-adduct formation was increased by only 2- and 1.5-fold, respectively. In conclusion, the increased efficacy of cisplatin nanocapsules in the cytotoxicity assay is due to increased platinum-DNA-adduct formation resulting from the enhanced cellular accumulation

Table 1. Cytotoxicity of cisplatin nanocapsules compared with free cisplatin in ovarian carcinoma cell lines

Cell line	IC_{50} free CisPt (mean ± SE; n = 3)	IC_{50} CisPt Nano (mean ± SE; n = 3)	Fold difference in IC_{50}
IGROV-1	0.10 ± 0.04	0.0011 ± 0.0005	100
SK-OV-3	2.37 ± 0.09	0.019 ± 0.001	125
A2780	1.61 ± 0.34	0.81 ± 0.03	2
OVCAR-3	0.41 ± 0.09	0.4 ± 0.11	1

NOTE: Cell survival was measured in a sulforhodamine B assay in response to increasing concentrations free and encapsulated cisplatin and IC_{50} values (μmol/L) were determined. In column 4, the ratios of the average IC_{50} value of free cisplatin over that of cisplatin nanocapsules are presented.

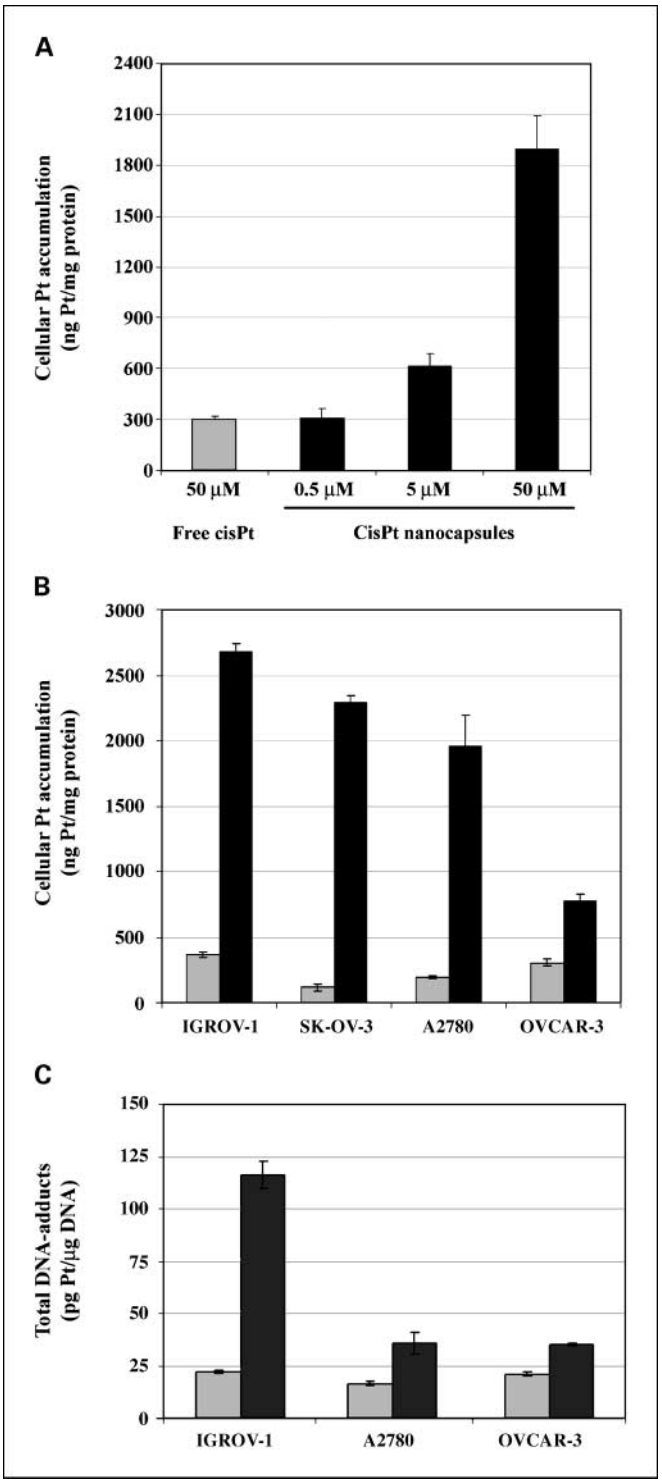

Fig. 1. Cellular accumulation and platinum-DNA-adduct formation in ovarian carcinoma cell lines after administration of cisplatin as free drug or as nanocapsules. *A,* total cellular accumulation of platinum in IGROV-1 cells treated for 2 h with 50 μmol/L free cisplatin (*gray column*) and 0.5, 5, and 50 μmol/L cisplatin (*CisPt*) nanocapsules (*black columns*). *Bars,* SD ($n = 3$). *B,* total cellular accumulation of platinum in a panel of human carcinoma cell lines treated for 2 h with 50 μmol/L free cisplatin (*gray columns*) and 50 μmol/L cisplatin nanocapsules (*black columns*). *Bars,* SD ($n = 3$). *C,* platinum-DNA-adduct formation in IGROV-1, A2780, and OVCAR-3 cells after treatment with cisplatin nanocapsules. DNA-coordinated platinum was measured after incubating cells for 4 h with 50 μmol/L free cisplatin (*gray columns*) or 50 μmol/L cisplatin in nanocapsules (*black columns*) and normalized for total DNA content (pg platinum/μg DNA). *Bars,* variation ($n = 2$).

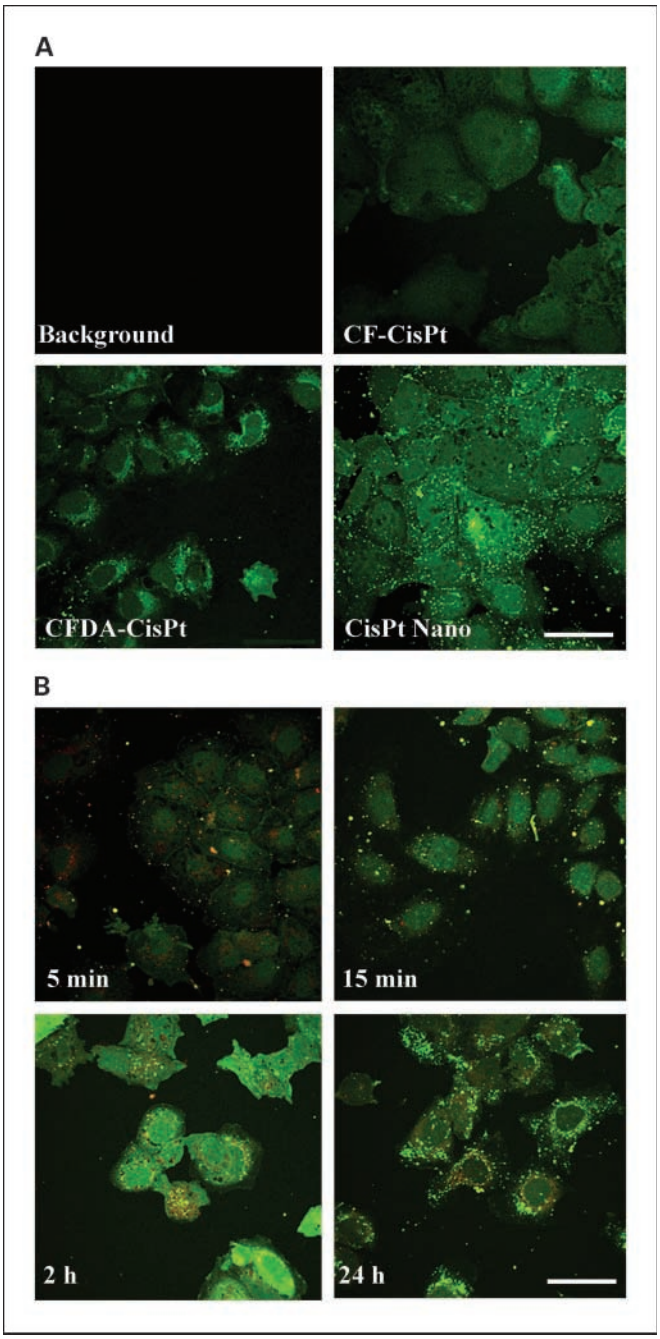

Fig. 2. Uptake of cisplatin nanocapsules visualized by fluorescence confocal microscopy. *A,* IGROV-1 cells were untreated (Background), incubated for 1 h with free cisplatin spiked with CF-cisplatin or CFDA-cisplatin, or incubated with CF-cisplatin-labeled nanocapsules (*CisPt Nano*) at a final cisplatin concentration of 50 μmol/L. Bar, 50 μm. *B,* IGROV-1 cells were incubated for 5 min, 15 min, 2 h (50 μmol/L cisplatin), or 24 h (5 μmol/L cisplatin) with double-labeled cisplatin nanocapsules. Note that the 24 h sample was treated with 5 μmol/L instead of 50 μmol/L cisplatin nanocapsules to avoid cell death. Bar, 50 μm.

of cisplatin. Moreover, there is a stronger correlation between cytotoxicity and DNA-adduct-formation than between cytotoxicity and cellular platinum accumulation. The high cellular accumulation of platinum in A2780 on the one hand (Fig. 1B) versus the low platinum-DNA-adduct formation on the other (Fig. 1C) suggests that in these cells the cisplatin accumulates at an intracellular location, where it is less toxic for the cells.

Cisplatin nanocapsules are taken up via endocytosis. To elucidate why the platinum accumulation, platinum-DNA-adduct formation, and cytotoxicity caused by the cisplatin nanocapsules are cell line dependent, we investigated the route of uptake and intracellular fate of fluorescently labeled cisplatin nanocapsules in IGROV-1, OVCAR-3, and A2780 cells using confocal fluorescence microscopy. The cisplatin core was labeled with 0.5 mol% CF-cisplatin, a fluorescent derivative of cisplatin that was previously used to investigate the intracellular localization of the free drug (14, 28). The phospholipid coat was labeled by inserting 0.2 mol% C5-Bodipy 581-PC, an acyl chain-labeled PC analogue exhibiting very slow spontaneous intermembrane exchange with a $t_{1/2}$ of 33 h (29). Introduction of the fluorescent labels did not affect the encapsulation efficiency and neither the cytotoxicity toward IGROV-1 cells (data not shown).

In IGROV-1 cells, the overall intracellular fluorescence was much higher in cells treated with cisplatin nanocapsules than in cells treated with the corresponding dose of free cisplatin spiked with 0.5 mol% CF-cisplatin or 0.5 mol% CFDA-cisplatin (Fig. 2A), showing that CF-cisplatin encapsulated in nanocapsules was taken up more efficiently than the free drug and its

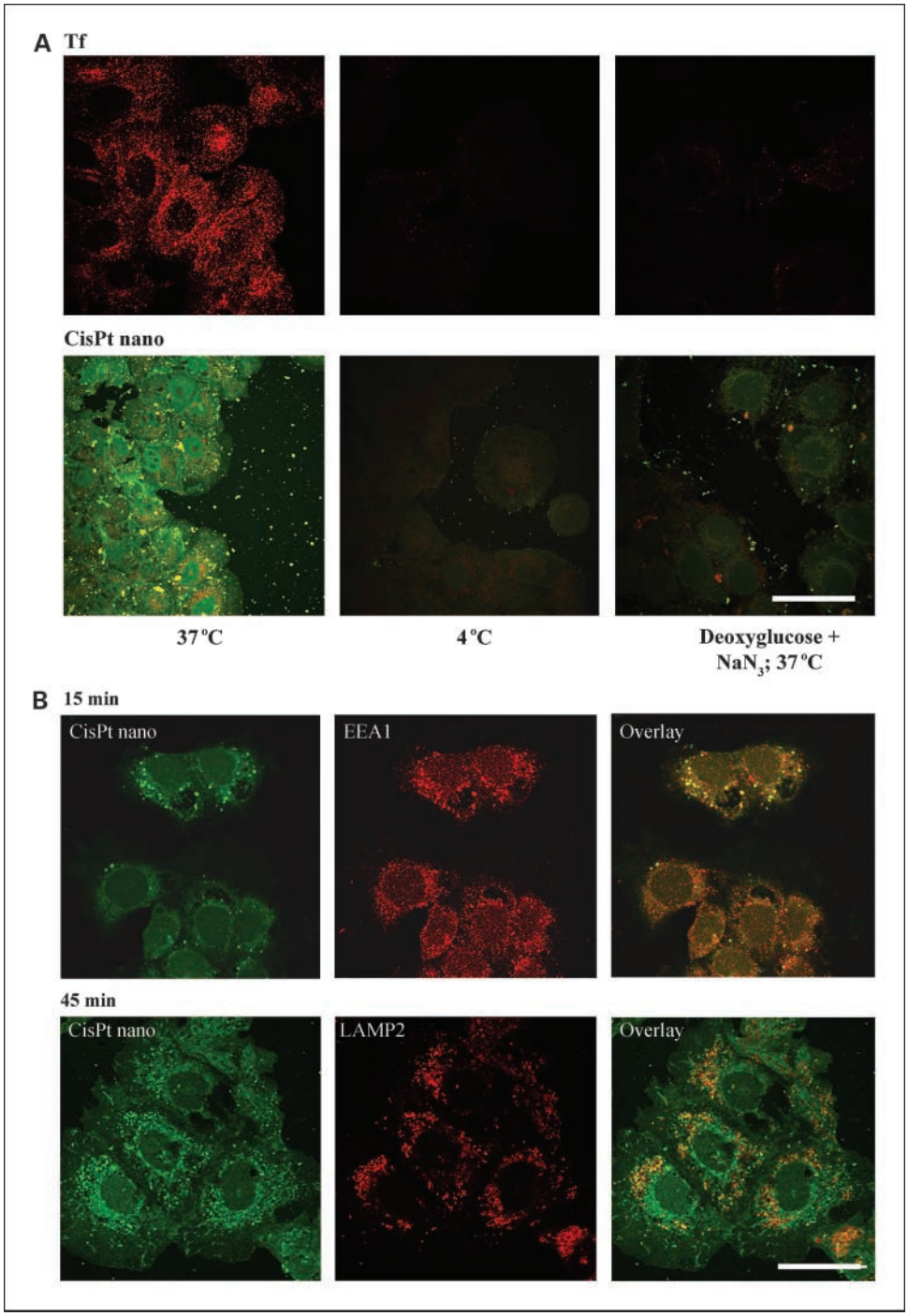

Fig. 3. Cisplatin nanocapsules are taken up via endocytosis. *A,* ATP-dependent processes in IGROV-1 cells were blocked by incubation at 4°C or by pretreatment of the cells with 50 mmol/L deoxyglucose and 10 mmol/L NaN_3. Cells were incubated for 60 min with double-labeled cisplatin nanocapsules to a final cisplatin concentration of 50 μmol/L or with 8 μmol/L Alexa Fluor 546-labeled transferrin (*Tf*) as a control. Bar, 50 μm. *B,* CF-cisplatin from nanocapsules colocalizes with early and late endosomes after uptake. IGROV-1 cells were incubated with CF-cisplatin-labeled cisplatin nanocapsules at a final cisplatin concentration of 50 μmol/L for 15 and 45 min, fixed, and costained for early endosomal antigen 1 (early endosomes) and lysosomal-associated membrane protein 2 (late endosomes and lysosomes), respectively. Bar, 50 μm.

nonpolar membrane permeable analogue (14, 28), respectively. The intracellular accumulation of CF-cisplatin from nanocapsules increases with time (Fig. 2B).

The localization of the fluorescent labels was found to change over time. At early time points (5 min-1 h), there is a high degree of colocalization of CF-cisplatin and C5-Bodipy 581-PC in the cells (Fig. 2B), suggesting that the uptake of cisplatin nanocapsules occurs via endocytosis. After 2 h, the colocalization is gradually lost (Fig. 2B; data not shown), and the fluorescence of CF-cisplatin changes from a uniform stain (2-8 h; Fig. 2B; data not shown) to a more punctate stain after 16 to 24 h (Fig. 2B; data not shown) that partially colocalizes with late endosomes/lysosomes and with parts of the Golgi network (Supplementary Fig. S1).

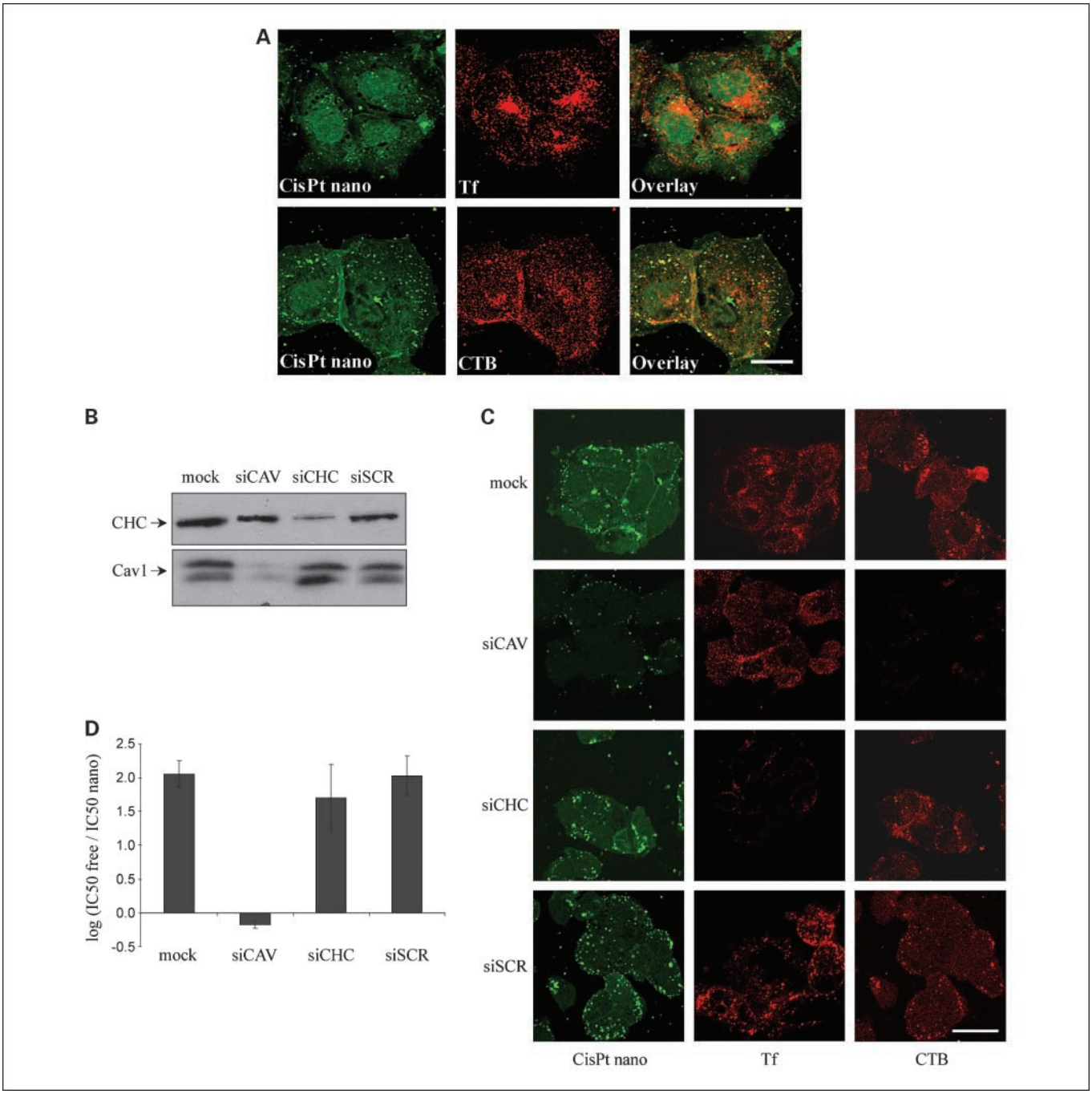

Fig. 4. Cisplatin nanocapsules are taken up via endocytosis mediated by caveolae. *A,* IGROV-1 cells were incubated for 15 min with CF-cisplatin-labeled nanocapsules and 10 μmol/L Alexa Fluor 546-labeled transferrin or 10 μmol/L Alexa Fluor 594-labeled CTB. Bar, 50 μm. *B,* Western blot detecting the expression of caveolin-1 (*Cav1*; double band due to two isoforms: Cav1A and B; ref. 34) and CHC in cell lysates of IGROV-1 that were mock-treated or treated with siRNA caveolin-1 (*siCAV*), siRNA CHC (*siCHC*), or siRNA scrambled control (*siSCR*) for 4 d. *C,* IGROV-1 cells were transfected with the siRNAs indicated and after 4 d incubated for 15 min with CF-cisplatin-labeled nanocapsules and 10 μmol/L Alexa Fluor 546-labeled transferrin or 10 μmol/L Alexa Fluor 594-labeled CTB. Bar, 50 μm. *D,* cell survival in response to increasing concentrations of cisplatin was measured for free and encapsulated cisplatin, and IC_{50} values were determined in IGROV-1 cells that had been mock-treated or treated with siCAV, siCHC, or siSCR for 4 d. Average ± variation log values of the ratios of the IC_{50} value of free cisplatin over that of cisplatin nanocapsules (n = 2).

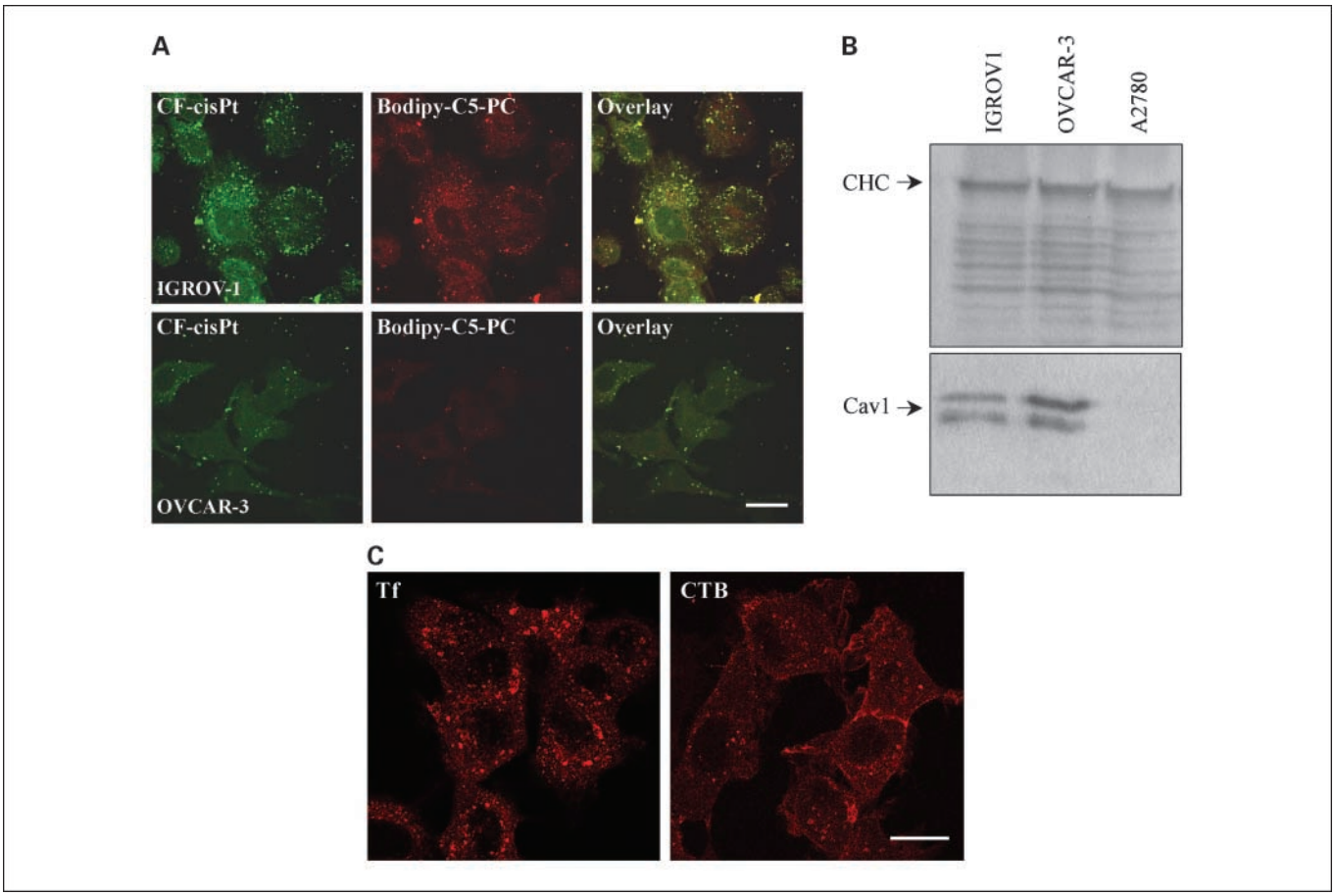

Fig. 5. Cisplatin nanocapsules are not taken up efficiently by OVCAR-3 cells. *A,* IGROV-1 and OVCAR-3 cells were incubated for 1 h with double-labeled nanocapsules to a final cisplatin concentration of 50 μmol/L, fixed, and mounted in Mowiol/Dabco. Bar, 25 μm. *B,* Western blot detecting the expression of caveolin-1 and CHC in cell lysates of IGROV-1, OVCAR-3, and A2780. *C,* OVCAR-3 cells were incubated for 15 min with 10 μmol/L Alexa Fluor 546-labeled transferrin or 10 μmol/L Alexa Fluor 594-labeled CTB fixed, and mounted in Mowiol/Dabco. Bar, 25 μm.

To address the involvement of endocytosis in the uptake of nanocapsules in IGROV-1 cells, all ATP-dependent processes were inhibited by incubating the cells at 4°C or by preincubation for 1 h with deoxyglucose and sodium azide. Under these conditions, the uptake of both Alexa Fluor 546-labeled transferrin, an established substrate of endocytosis (20), and cisplatin nanocapsules is inhibited (Fig. 3A), showing that the uptake of cisplatin nanocapsules is energy dependent. Further evidence for the uptake of nanocapsules via endocytosis was provided by the colocalization of CF-cisplatin from nanocapsules with early endosomal antigen 1 (30) and lysosomal-associated membrane protein 2 (staining late endosomes and lysosomes; ref. 31; Fig. 3B).

Caveolin-1 expression is essential for uptake and increased cytotoxic effect of cisplatin nanocapsules in IGROV-1. Several endocytic pathways have been identified that internalize particles with a diameter of 50 to 300 nm, including clathrin- and caveolae-mediated endocytosis (32). To investigate the involvement of these pathways in the uptake of the nanocapsules in IGROV-1 cells, co-uptake experiments with cholera toxin B (CTB)-Alexa Fluor 594, a marker for caveolae-mediated endocytosis (33), and transferrin-Alexa Fluor 546, a marker for clathrin-mediated endocytosis (20), were done (Fig. 4A). Interestingly, the CF-cisplatin-labeled nanocapsules predominantly colocalize with CTB during uptake, whereas only a few spots of nanocapsule-transferrin colocalization were observed, indicating that the nanocapsules are taken up via caveolae rather than via clathrin-coated pits.

Subsequently, we used various siRNAs to specifically inhibit the endocytic pathways (Fig. 4B-D; Supplementary Fig. S2): the clathrin-coated vesicle pathway was inhibited by down-regulating the CHC (siCHC) and the caveolin route was inhibited by the silencing of caveolin-1 (siCAV). In the control experiments, a scrambled siRNA (siSCR) was used. The uptake of CTB and transferrin was monitored in parallel to verify the effective inactivation of caveolae- and clathrin-mediated endocytosis, respectively. In caveolin-1 knockdown cells, the uptake of fluorescent nanocapsules is completely blocked, whereas the nanocapsules are efficiently endocytosed by the CHC knockdown cells and the cells treated with siSCR (Fig. 4C).

To directly address the role of caveolae-mediated uptake in the cytotoxicity of nanocapsules in IGROV-1 cells, the expression of either caveolin-1 or CHC was reduced by siRNA and the cytotoxicity of the nanocapsules was compared with that of free cisplatin (Fig. 4D). In the CHC knockdown cells and in the cells treated with siSCR, the cytotoxicity of the nanocapsules is not significantly affected compared with the

mock-treated cells. In contrast, the cytotoxicity of the nanocapsules was reduced to that of free cisplatin in cells with down-regulated caveolin-1 (Fig. 4D). The IC_{50} value of the free drug was not affected by the siRNA treatments (data not shown). In conclusion, our data show that both the uptake and the cytotoxic effect of cisplatin nanocapsules are abrogated by down-regulating caveolin-1 expression, showing that the uptake of nanocapsules by IGROV-1 cells proceeds predominantly by caveolae-mediated endocytosis, which is required for the cytotoxic effect of the nanocapsules.

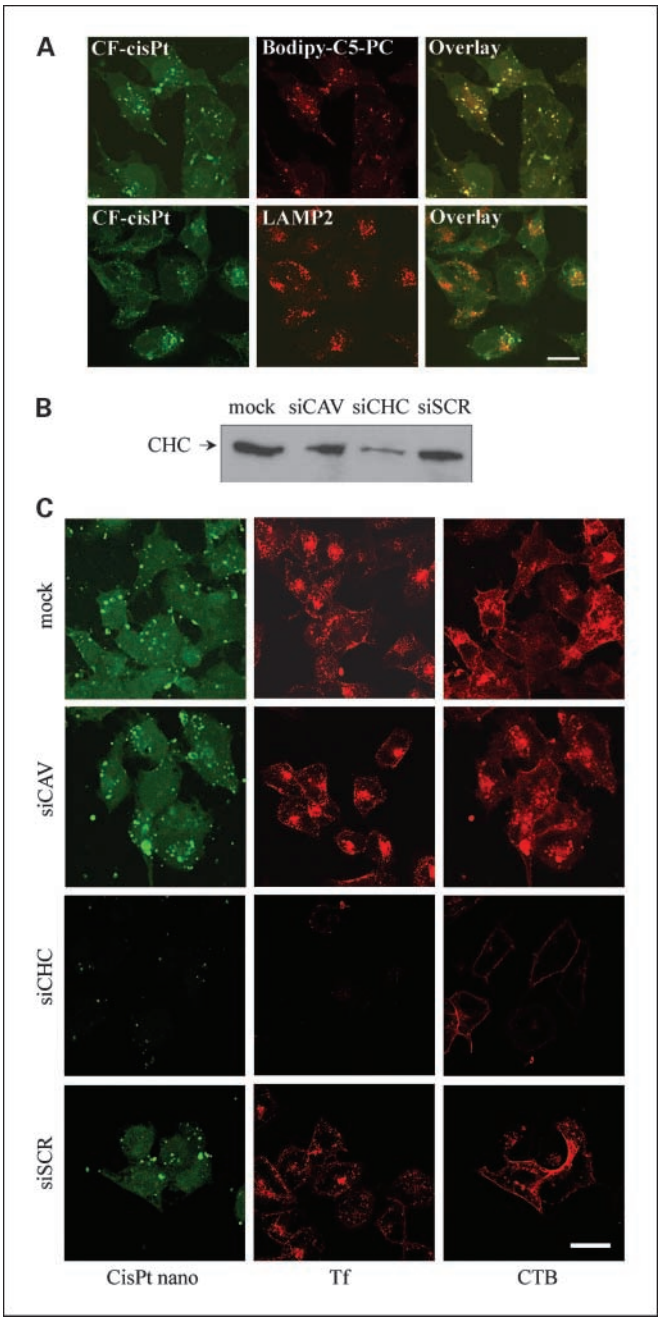

Fig. 6. Cisplatin nanocapsules are taken up very efficiently via clathrin-mediated endocytosis in A2780 cells and accumulate in the endosomal compartment. *A,* A2780 cells were incubated for 1 h with double-labeled (*top*) or CF-cisplatin-labeled nanocapsules (*bottom*) to a final cisplatin concentration of 50 μmol/L, fixed, and mounted in Mowiol/Dabco. The cells treated with CF-cisplatin nanocapsules were costained for lysosomal-associated membrane protein 2 (late endosomes/lysosomes) after fixation. Bar, 25 μm. *B,* Western blot detecting the expression of CHC in cell lysates of A2780 that were mock-treated or treated with siCAV, siCHC, or siSCR for 4 d. *C,* A2780 cells were transfected with the siRNAs indicated and after 4 d incubated for 15 min with CF-cisplatin-labeled nanocapsules and 10 μmol/L Alexa Fluor 546-labeled transferrin or 10 μmol/L Alexa Fluor 594-labeled CTB. Bar, 25 μm.

Differences in efficacy of cisplatin nanocapsules are due to differences in trafficking. We hypothesized that the lack of a strongly enhanced cytotoxic effect of the nanocapsules compared with the free drug in the OVCAR-3 and A2780 cells was due to differences in uptake. As shown above, OVCAR-3 cells exhibited only slightly increased cellular platinum accumulation and formation of platinum-DNA-adducts on exposure to cisplatin nanocapsules (Fig. 1B and C). Accordingly, the uptake of fluorescent nanocapsules was strongly reduced in the OVCAR-3 cells when compared with the uptake of cisplatin nanocapsules in IGROV-1 cells (Fig. 5A). The cause for this reduced internalization is currently not known. It is not due to reduced expression of either caveolin-1 or CHC (Fig. 5B), and neither to a defect in the endocytic pathways, because both transferrin and CTB are internalized in OVCAR-3 cells (Fig. 5C).

In A2780 cells, CF-cisplatin and C5-Bodipy 581-PC are found in distinct large endosomal structures in the cytoplasm 1 h after adding fluorescent nanocapsules (Fig. 6A). The partial colocalization of CF-cisplatin with lysosomal-associated membrane protein 2 in A2780 suggests that the nanocapsules accumulate in late endosomes/lysosomes (Fig. 6A). The high intracellular platinum accumulation (Fig. 1B) in A2780 cells and the virtual absence of expression of caveolin-1 (Fig. 5B) implicate an alternative caveolin-1 independent route of uptake. Co-uptake experiments revealed colocalization of nanocapsules with both CTB and transferrin in A2780 cells (Supplementary Fig. S3, mock-treated cells), indicating that the nanocapsules and CTB are taken up via clathrin-mediated endocytosis. The partial colocalization with transferrin (Supplementary Fig. S3) suggests that nanocapsules become trapped in the recycling compartment (35). Subsequent siRNA knockdown experiments in A2780 cells confirmed the specific uptake via the formation of clathrin-coated vesicles (Fig. 6B and C; Supplementary Fig. S3). The cell entry via clathrin-coated pits and subsequent accumulation of the nanocapsules in a late endosomal/lysosomal compartment, from which cisplatin is hardly released, explain the apparent discrepancy between the cellular platinum accumulation and the platinum-DNA-adduct formation data in the A2780 cells. The results suggest that cisplatin nanocapsules are only effective after endocytosis via a caveolin-1-dependent mechanism and subsequent routing to a compartment from which cisplatin can escape.

Discussion

In this study, we have shown that the strongly increased *in vitro* cytotoxicity of cisplatin nanocapsules compared with the free drug in IGROV-1 cells (11) results from uptake of the nanocapsules by caveolae-mediated endocytosis leading to increased intracellular accumulation of cisplatin and increased levels of platinum-DNA-adducts. The extent of the increase in cytotoxicity of cisplatin nanocapsules over that of the free drug showed a strong cell line dependence and was largest for the IGROV-1 and SK-OV-3 cells. In OVCAR-3 cells, the nanocapsules are as cytotoxic as the free drug, which is attributed to the virtual absence of internalization of the nanocapsules. In

A2780 cells, which lack caveolin-1, the cisplatin nanocapsules are taken up via clathrin-mediated endocytosis and become trapped in an endocytic compartment, resulting in only modest increases in platinum-DNA-adduct formation and toxicity of the encapsulated versus the free drug.

Following the caveolar uptake of the nanocapsules by IGROV-1 cells, cisplatin escapes from the endosomal compartments as evidenced by the cytosolic localization of the CF-cisplatin and the formation of DNA-adducts. At later time points (8-24 h after addition), the majority of the CF-cisplatin was found to colocalize with markers of the Golgi network and late endosomes/lysosomes, as was also observed after administration of CFDA-cisplatin (14, 28, 36). This suggests that cisplatin from nanocapsules, although it is taken up via a different route and accumulates at much higher levels in the cells, is processed similarly to the drug taken up from solution. A minor part of the cisplatin binds to DNA (1), whereas the majority is removed from the cell by the copper transporters ATP7A and ATP7B in the trans-Golgi network (14, 28, 36).

In the OVCAR-3 and A2780 cell lines, in which the nanocapsules do not exert a strongly enhanced cytotoxic effect compared with the free drug, the cisplatin from nanocapsules does not reach the nucleus to form platinum-DNA-adducts. In OVCAR-3 cells, this is caused by a lack of internalization of cisplatin nanocapsules. OVCAR-3 cells were reported previously to have a low capacity to bind to and internalize phospholipid vesicles, limiting the *in vitro* potency of liposomes in these cells (37). As OVCAR-3 does take up CTB and transferrin, the inability to internalize the nanocapsules is likely due to a lack of binding to the cell surface, suggesting that uptake could be accomplished by attaching an appropriate ligand to the nanocapsules (38). Recently, the cisplatin nanocapsules were tested *in vivo* in nude mice bearing OVCAR-3 carcinoma xenografts (39). The cisplatin nanocapsules were found to have similar antitumor activity as free cisplatin, consistent with the present *in vitro* data.

In A2780 cells, the cisplatin nanocapsules are efficiently taken up; however, they do not lower the IC_{50} value of cisplatin by 2 orders of magnitude as in IGROV-1 and SK-OV-3 cells. This is attributed to a lack of cisplatin release from the endocytic compartment in which the nanocapsules accumulate. In contrast to IGROV-1, A2780 does not express caveolin-1 and internalizes nanocapsules as well as CTB by clathrin-mediated endocytosis. This observation is in agreement with previous studies showing endocytosis of CTB by clathrin-dependent endocytosis in various cell types (40). Further research is required to clarify why cisplatin does not escape from the endosomes in A2780 cells. Possibly, this is due to the route of cell entry, with uptake via clathrin-mediated endocytosis resulting in a different intracellular processing of the nanocapsules than uptake by caveolae-mediated endocytosis.

The virtually exclusive uptake of nanocapsules by caveolar endocytosis in IGROV-1 cells is an unexpected observation. Thus far, only the SV40 virus has been reported to be taken up exclusively via caveolae in CV-1 cells using MHC class I proteins as cell-surface receptor (41). Few studies have reported endocytosis of liposomes by tumor cells (42, 43), and to our knowledge, only one study has evaluated the involvement of different endocytic pathways in the uptake of liposomes (44). Huth et al. have shown that multiple pathways are involved in uptake of pH-sensitive liposomes with the relative contributions varying between cell lines. HUVEC seem to internalize via clathrin-dependent endocytosis, caveolae-dependent endocytosis, and macropinocytosis, whereas in COS-7 cells macropinocytosis is not involved in the uptake (44). For lipoplexes, aggregates of positively charged lipids with nucleic acids, including genes, siRNA, and antisense RNA, the mechanisms of internalization by cells have been studied more extensively, and a variety of endocytic pathways has been implicated including phagocytosis, macropinocytosis, clathrin-mediated and non-clathrin-mediated endocytosis, and entry via caveolae (45). Recently, lipoplexes were reported to be preferentially taken up in CHO cells by either the clathrin-mediated or the caveolin-mediated route depending on the cationic surfactant used to make the lipoplexes (46).

At this point, we can only speculate about the origin of the selective internalization of nanocapsules by caveolar endocytosis in IGROV-1 cells. Particle size has been reported to determine the route of cellular entry. However, the size dependence for uptake by caveolae or clathrin-coated vesicles was found to vary with the nature of the particles and/or the cell types studied (32, 47). The nanocapsules fall in a size range that is compatible with both routes of uptake. Particles with a lipid composition similar to that of the nanocapsules and with a homogeneous size distribution, 1,2-dioleoyl-*sn*-glycero-3-phosphocholine/1,2-dioleoyl-*sn*-glycero-3-phosphoserine (1:1) vesicles extruded through 200 nm pore filters (LUVET200), are also taken up via the caveolar pathway in IGROV-1 cells,[5] indicating that the shape and rigidity of a particle are not determining factors. Possibly, the surface charge of the particles is important for directing the nanocapsules to caveolae.

With the recent demonstration by intravital microscopy that liposomes can be endocytosed by tumor cells in tumor tissue *in vivo* (48), the present study may also bear on the clinical application of cisplatin. The dependence of the cytotoxicity on the route of cellular entry established for cisplatin nanocapsules may provide a new strategy for predicting the efficacy of nanoparticulate anticancer drug delivery systems against different types of tumors. A major cause of cisplatin resistance in cancer cell lines and tumors is known to be reduced drug uptake (49). The cisplatin nanocapsules may circumvent the mechanisms leading to the reduced drug accumulation and thus kill the platinum-resistant cells. Recent data suggest that nanocapsules can overcome platinum resistance *in vitro* (50).[6]

Disclosure of Potential Conflicts of Interest

No potential conflicts of interest were disclosed.

Acknowledgments

We thank Prof. Dr. J. Schellens (Dutch Cancer Institute) and B. Hendriks (University Medical Center Utrecht) for help with the measurements of cellular platinum accumulation and platinum-DNA-adducts, Drs. Tobias Dansen and Maria Velinova for performing the pilot confocal fluorescence microscopy experiments, Drs. R. Heetebrij and G. Kalayda for generously providing CFDA-cisplatin samples, and Dr. Rob Roovers for advice and for providing antibodies for the endosome and endoplasmic reticulum colocalization studies.

[5] Our unpublished results.

[6] I.H.L. Hamelers, unpublished data.

References

1. Ho YP, Au-Yeung SC, To KK. Platinum-based anticancer agents: innovative design strategies and biological perspectives. Med Res Rev 2003;23:633–55.
2. Wernyj RP, Morin PJ. Molecular mechanisms of platinum resistance: still searching for the Achilles' heel. Drug Resist Updat 2004;7:227–32.
3. Harrington KJ, Syrigos KN, Vile RG. Liposomally targeted cytotoxic drugs for the treatment of cancer. J Pharm Pharmacol 2002;54:1573–600.
4. Harrington KJ, Lewanski CR, Northcote AD, et al. Phase I-II study of pegylated liposomal cisplatin (SPI-077) in patients with inoperable head and neck cancer. Ann Oncol 2001;12:493–6.
5. Meerum Terwogt JM, Groenewegen G, Pluim D, et al. Phase I and pharmacokinetic study of SPI-77, a liposomal encapsulated dosage form of cisplatin. Cancer Chemother Pharmacol 2002;49:201–10.
6. White SC, Lorigan P, Margison GP, et al. Phase II study of SPI-77 (sterically stabilised liposomal cisplatin) in advanced non-small-cell lung cancer. Br J Cancer 2006;95:822–8.
7. Stathopoulos GP, Boulikas T, Vougiouka M, et al. Pharmacokinetics and adverse reactions of a new liposomal cisplatin (Lipoplatin): phase I study. Oncol Rep 2005;13:589–95.
8. Bandak S, Goren D, Horowitz A, Tzemach D, Gabizon A. Pharmacological studies of cisplatin encapsulated in long-circulating liposomes in mouse tumor models. Anticancer Drugs 1999;10:911–20.
9. Riley CM, Sternson LA. Cisplatin. In: Florey K, editor. Analytical profiles of drug substances. Vol. 14. New York: Academic Press; 1985. p. 78–105.
10. Burger KN, Staffhorst RW, de Vijlder HC, et al. Nanocapsules: lipid-coated aggregates of cisplatin with high cytotoxicity. Nat Med 2002;8:81–4.
11. Chupin V, de Kroon AI, de Kruijff B. Molecular architecture of nanocapsules, bilayer-enclosed solid particles of cisplatin. J Am Chem Soc 2004;126:13816–21.
12. Velinova MJ, Staffhorst RW, Mulder WJ, et al. Preparation and stability of lipid-coated nanocapsules of cisplatin: anionic phospholipid specificity. Biochim Biophys Acta 2004;1663:135–42.
13. De Kroon AI, Staffhorst RW, de Kruijff B, Burger KN. Cisplatin nanocapsules. Methods Enzymol 2005;391:118–25.
14. Molenaar C, Teuben JM, Heetebrij RJ, Tanke HJ, Reedijk J. New insights in the cellular processing of platinum antitumor compounds, using fluorophore-labeled platinum complexes and digital fluorescence microscopy. J Biol Inorg Chem 2000;5:655–65.
15. Skehan P, Storeng R, Scudiero D, et al. New colorimetric cytotoxicity assay for anticancer-drug screening. J Natl Cancer Inst 1990;82:1107–12.
16. Bradford MM. A rapid and sensitive method for the quantitation of microgram quantities of protein utilizing the principle of protein-dye binding. Anal Biochem 1976;72:248–54.
17. Ma J, Verweij J, Kolker HJ, van Ingen HE, Stoter G, Schellens JH. Pharmacokinetic-dynamic relationship of cisplatin *in vitro*: simulation of an i.v. bolus and 3 h and 20 h infusion. Br J Cancer 1994;69:858–62.
18. Roovers RC, Laeremans T, Huang L, et al. Efficient inhibition of EGFR signalling and of tumour growth by antagonistic anti-EGFR Nanobodies. Cancer Immunol Immunother 2006;56:303–17.
19. de Graaf P, Zwart WT, van Dijken RA, et al. Phosphatidylinositol 4-kinase β is critical for functional association of rab11 with the Golgi complex. Mol Biol Cell 2004;15:2038–47.
20. Stoorvogel W, Kerstens S, Fritzsche I, et al. Sorting of ligand-activated epidermal growth factor receptor to lysosomes requires its actin-binding domain. J Biol Chem 2004;279:11562–9.
21. Hamelers IH, Olivo C, Mertens AE, et al. The Rac activator Tiam1 is required for $\alpha 3\beta 1$-mediated laminin-5 deposition, cell spreading, and cell migration. J Cell Biol 2005;171:871–81.
22. Cho KA, Ryu SJ, Park JS, et al. Senescent phenotype can be reversed by reduction of caveolin status. J Biol Chem 2003;278:27789–95.
23. Motley A, Bright NA, Seaman MN, Robinson MS. Clathrin-mediated endocytosis in AP-2-depleted cells. J Cell Biol 2003;162:909–18.
24. Kelland LR, Jones M, Abel G, Valenti M, Gwynne J, Harrap KR. Human ovarian-carcinoma cell lines and companion xenografts: a disease-oriented approach to new platinum anticancer drug discovery. Cancer Chemother Pharmacol 1992;30:43–50.
25. Roberts D, Schick J, Conway S, et al. Identification of genes associated with platinum drug sensitivity and resistance in human ovarian cancer cells. Br J Cancer 2005;92:1149–58.
26. Rixe O, Ortuzar W, Alvarez M, et al. Oxaliplatin, tetraplatin, cisplatin, and carboplatin: spectrum of activity in drug-resistant cell lines and in the cell lines of the National Cancer's Institute Anticancer Drug Screen Panel. Biochem Pharmacol 1996;52:1855–65.
27. Ma J. Clinical and preclinical pharmacokinetic and dynamic studies with cisplatin, topotecan and docetaxel. Ph.D. thesis. Rotterdam (The Netherlands): Medical Oncology, Erasmus University; 1996.
28. Safaei R, Katano K, Larson BJ, et al. Intracellular localization and trafficking of fluorescein-labeled cisplatin in human ovarian carcinoma cells. Clin Cancer Res 2005;11:756–67.
29. Elvington SM, Nichols JW. Spontaneous, intervesicular transfer rates of fluorescent, acyl chain-labeled phosphatidylcholine analogs. Biochim Biophys Acta 2007;1768:502–8.
30. Mu FT, Callaghan JM, Steele-Mortimer O, et al. EEA1, an early endosome-associated protein. EEA1 is a conserved α-helical peripheral membrane protein flanked by cysteine "fingers" and contains a calmodulin-binding IQ motif. J Biol Chem 1995;270:13503–11.
31. Chen JW, Murphy TL, Willingham MC, Pastan I, August JT. Identification of two lysosomal membrane glycoproteins. J Cell Biol 1985;101:85–95.
32. Rejman J, Oberle V, Zuhorn IS, Hoekstra D. Size-dependent internalization of particles via the pathways of clathrin- and caveolae-mediated endocytosis. Biochem J 2004;377:159–69.
33. Kirkham M, Parton RG. Clathrin-independent endocytosis: new insights into caveolae and non-caveolar lipid raft carriers. Biochim Biophys Acta 2005;1745:273–86.
34. Razani B, Lisanti MP. Caveolin-deficient mice: insights into caveolar function human disease. J Clin Invest 2001;108:1553–61.
35. McGraw TE, Dunn RW, Maxfield FR. Isolation of a temperature-sensitive variant Chinese hamster ovary cell line with a morphologically altered endocytic recycling compartment. J Cell Physiol 1993;155:579–94.
36. Katano K, Safaei R, Samimi G, et al. Confocal microscopic analysis of the interaction between cisplatin and the copper transporter ATP7B in human ovarian carcinoma cells. Clin Cancer Res 2004;10:4578–88.
37. Straubinger RM, Lopez NG, Debs RJ, Hong K, Papahadjopoulos D. Liposome-based therapy of human ovarian cancer: parameters determining potency of negatively charged and antibody-targeted liposomes. Cancer Res 1988;48:5237–45.
38. Torchilin VP. Multifunctional nanocarriers. Adv Drug Deliv Rev 2006;58:1532–55.
39. Staffhorst RW, van der Born K, Erkelens CA, et al. Antitumor activity and biodistribution of cisplatin nanocapsules in nude mice bearing human ovarian carcinoma xenografts. Anticancer Drugs 2008;19:721–7.
40. Torgersen ML, Skretting G, van Deurs B, Sandvig K. Internalization of cholera toxin by different endocytic mechanisms. J Cell Sci 2001;114:3737–47.
41. Pelkmans L, Kartenbeck J, Helenius A. Caveolar endocytosis of simian virus 40 reveals a new two-step vesicular-transport pathway to the ER. Nat Cell Biol 2001;3:473–83.
42. Lakkaraju A, Rahman YE, Dubinsky JM. Low-density lipoprotein receptor-related protein mediates the endocytosis of anionic liposomes in neurons. J Biol Chem 2002;277:15085–92.
43. Torchilin VP, Rammohan R, Weissig V, Levehenko TS. TAT peptide on the surface of liposomes affords their efficient intracellular delivery even at low temperature and in the presence of metabolic inhibitors. Proc Natl Acad Sci U S A 2001;98:8786–91.
44. Huth US, Schubert R, Peschka-Suss R. Investigating the uptake and intracellular fate of pH-sensitive liposomes by flow cytometry and spectral bioimaging. J Control Release 2006;110:490–504.
45. Khalil IA, Kogure K, Akita H, Harashima H. Uptake pathways and subsequent intracellular trafficking in nonviral gene delivery. Pharmacol Rev 2006;58:32–45.
46. Wong AW, Scales SJ, Reilly DE. DNA internalized via caveolae requires microtubule-dependent, Rab7-independent transport to the late endocytic pathway for delivery to the nucleus. J Biol Chem 2007;282:22953–63.
47. Grosse S, Aron Y, Thevenot G, Francois D, Monsigny M, Fajac I. Potocytosis and cellular exit of complexes as cellular pathways for gene delivery by polycations. J Gene Med 2005;7:1275–86.
48. Seynhaeve AL, Hoving S, Schipper D, et al. Tumor necrosis factor α mediates homogeneous distribution of liposomes in murine melanoma that contributes to a better tumor response. Cancer Res 2007;67:9455–62.
49. Kelland LR. Preclinical perspectives on platinum resistance. Drugs 2000;59:1–8; discussion 37–8.
50. Helleman J, Burger H, Hamelers IH, et al. Impaired cisplatin influx in an A2780 mutant cell line: evidence for a putative, *cis*-configuration-specific, platinum influx transporter. Cancer Biol Ther 2006;5:943–9.